



Revue des Sciences et Sciences de l'ingénieur

Journal of sciences and engineering sciences

ISSN 2170-0737 EISSN: 2600-7029

<https://www.asjp.cerist.dz/en/PresentationRevue/303>



Comparative Numerical Simulation Between p and n-type Substrate of Heterojunction with Intrinsic Silicon Solar Cell

Zarede Toufik^{1,2}, Lidjici Hamza^{2,*}, Zoukel Abdelhalim³ and Mahrane Achour¹

¹Unité de Développement des Equipements Solaire. UDES/Centre de Développement des Energies Renouvelable. CDER Bou Ismail. 42415. W. Tipaza, Algérie.

²Laboratoire d'étude et de Développement de Matériaux Semiconducteurs et Diélectrique, Université de Laghouat, route de Ghardaïa, BP37G, Laghouat, Algérie.

³Laboratoire physico-chimie des matériaux, Université de Laghouat, route de Ghardaïa, BP37G, Laghouat, Algérie.

Article history

Received: 2019-04-17

Accepted: 2019-05-12

Abstract

This work presents a comparative numerical simulation between p and n- type substrate of the heterojunction with intrinsic silicon solar cell. The first heterojunction with intrinsic in silicon solar cell is composed with 100 μm of silicon p-type wafer with $1,5 \cdot 10^{16} \text{ cm}^{-3}$ acceptor concentration, and the second heterojunction with intrinsic in silicon structure is composed with 100 μm of silicon n-type wafer with $1,5 \cdot 10^{16} \text{ cm}^{-3}$ donor concentration, The effective average electron and hole lifetime for the substrate p or n considered in our modeling they are equal. A high photovoltaic efficiency conversion is about 21.43% for p-type wafer and 22.8% for n-type wafer was obtained.

Key-words: Silicon, Heterojunction, Solar cell.

Résumé

Ce travail présente une comparaison par simulation numérique entre les deux cellules solaires à hétérojonction en silicium, la première avec substrat de type p et la deuxième avec substrat de type n. La première cellule solaire à hétérojonction de silicium est composée de 100 μm de substrat de silicium de type p avec une concentration de $1,5 \cdot 10^{16} \text{ cm}^{-3}$, et la seconde cellule est composée de 100 μm de substrat de silicium de type n avec une concentration de $1,5 \cdot 10^{16} \text{ cm}^{-3}$. Un rendement de conversion photovoltaïque élevée d'environ 21,43% pour le silicium de type p, et de 22,8% pour le silicium de type n a été obtenu.

Mots-clés : Silicium, Hétérojonction, Cellule solaire.

* Corresponding author. Tel./fax: +213 0773165764.

E-mail address: h.lidjici@lagh-univ.dz

1. Introduction

Today the technology of electricity production from solar photovoltaic cells a promising way for the development of our country.

The numerical modeling and simulation is increasingly used in many technological and scientific sectors. Numerical modeling has been applied to silicon solar cells since the early days of computer modeling and has recently become widely used in the photovoltaic's industry [1].

The software calculation codes generally use the finite element method. This method solves the partial differential equations, which correspond to the mathematical laws of simulated physical phenomena[2][3].

The heterojunction of silicon solar with intrinsic thin layer of amorphous silicon cell named HIT is promoter for cells with high photovoltaic conversion efficiency [4][5].

The HIT silicon solar cell consist of an n or p-doped c-Si crystalline silicon base and a Very thin layer of amorphous silicon (a-Si) of the p or n type, this type of cell, has a low temperature deposition process (<200°C) and the symmetrical structure of HIT cells can suppress thermal and mechanical stress during its production process and results in an advantage for thinner crystalline silicon wafers [6].

We propose in this work a contribution to the modeling and simulation by comparative study between p an n-type substrate of heterojunction with intrinsic thin layer silicon solar cell.

2. Solar cell modeling

The modeling and simulation in 1D using AFORS-HET is based on the numerical solution of the three fundamental equations of charge transport in semiconductors in one dimension. Which are respectively the Poisson equation and the continuity equation for electrons and holes. In AFORS HET the Poisson equation is expressed by the following relationship [7]:

$$\frac{\epsilon_0 \epsilon_r}{q} \frac{\partial^2 \phi(x)}{\partial x^2} = p(x) - n(x) + N_D - N_A + \sum_{defects} \rho_t(x)$$

Along with:

Acceptor defect density is:

$$\rho(x) = - \int dE f(E, x) N_i(E)$$

Donor type defect density is:

$$\rho(x) = \int dE (1 - f(E, x)) N(E)$$

ϵ_0 : absolute dielectric constant.

ϵ_r : relative dielectric constant.

ϕ : electrostatic potential.

q : electron charge.

n/p : electron/hole.

N_D/N_A : concentrations of the donors/acceptors.

The charge stored in the defects is described by a distribution function f_t .

The continuity equations are expressed by :

For electrons:

$$-\frac{1}{q} \frac{\partial j_n(x)}{\partial x} = G_n(x) - R_n(x) - \frac{\partial}{\partial t} n(x)$$

For holes:

$$\frac{1}{q} \frac{\partial j_p(x)}{\partial x} = G_p(x) - R_p(x) - \frac{\partial}{\partial t} p(x)$$

Along with:

$J_{n,p}$ is the electron current density and holes.

$G_{n,p}$ is the generation rate of electron and hole.

$R_{n,p}$ is the rate of recombination electron hole.

The densities of carriers are calculated by the model Drift-Diffusion, this model is based on the expression of electron and hole densities J_n, J_p following [8]:

$$j_n(x) = q \mu_n n(x) \frac{\partial E_{Fn}(x)}{\partial x} = -\frac{\mu_n kT}{q} \frac{\partial n(x)}{\partial x} + \mu_n n(x) \frac{\partial \phi(x)}{\partial x}$$

$$j_p(x) = q \mu_p p(x) \frac{\partial E_{Fp}(x)}{\partial x} = -\frac{\mu_p kT}{q} \frac{\partial p(x)}{\partial x} - \mu_p p(x) \frac{\partial \phi(x)}{\partial x}$$

$F_{n,p}$ the Fermi levels.

$\mu_{n,p}$ mobilities of electrons and holes.

In the case of modeling and simulation in equilibrium or stationary calculation mode, the time t disappears in the partial derivatives, which leads to a simplified system of differential equations with functions dependent only on the position x .

The boundary conditions using in simulation by AFORS-HET[9]:

- the electrostatic potential at $x=0$:

$$\phi(0) = \phi_{front} - \phi_{back} + V_{ext}$$

$$j_n(0) = q S_n^{front} (n(0) - n_{eq}(0))$$

$$j_p(0) = -q S_p^{front} (p(0) - p_{eq}(0))$$

- the potential at $x=L$:

$$\phi(L) = 0$$

$$j_n(L) = -q S_n^{back} (n(L) - n_{eq}(L))$$

$$j_p(L) = q S_p^{back} (p(L) - p_{eq}(L))$$

Where:

L : thickness of the cell between front and back contact.

ϕ : metal work function.

V_{ext} : applied voltage.

$$n_{eq} = N_C e^{-\frac{q\phi - q\chi}{kT}}$$

$$p_{eq} = N_V e^{-\frac{E_g - q\phi + q\chi}{kT}}$$

X: affinity in eV.

E_g : band gap.

AFORS-Het solves numerically the one-dimensional semiconductor equations with the appropriate boundary conditions in order to transform the coupled partial differential equations into a set of nonlinear algebraic equations by the finite difference method with discretization by the iteration algorithms Newton-Raphson, and leads to a nonlinear system with simple Jacobian structure that can be solved efficiently by the Newton-Raphson technique[7][10].

3. Solar cell definition

The physical parameters of the HIT cell p-type substrate to be simulated under the AFORS-HET 1D software are given in Table I:

| Paramètres | c-Si(p) | a-Si(n) | a-Si(p) |
|--|-----------------------|----------------------|----------------------|
| Thickness | 100µm | 5nm | 5nm |
| Dielectric constant | 11.9 | 11.9 | 11.9 |
| Electron affinity (eV) | 4.05 | 3.9 | 3.9 |
| Bandgap (eV) | 1.12 | 1.72 | 1.72 |
| Effective conduction band density(cm ⁻³) | 2.8x10 ¹⁹ | 10 ²⁰ | 10 ²⁰ |
| Effective valence band density(cm ⁻³) | 2.6x10 ¹⁹ | 10 ²⁰ | 10 ²⁰ |
| Electron mobility(cm ² V ⁻¹ s ⁻¹) | 1041 | 20 | 20 |
| Hole mobility (cm ² V ⁻¹ s ⁻¹) | 412 | 5 | 5 |
| Acceptor concentration(cm ⁻³) | 0 | 0 | 6.8x10 ¹⁹ |
| Donor concentration(cm ⁻³) | 1.5x10 ¹⁶ | 6.8x10 ¹⁹ | 0 |
| Thermal velocity of electrons(cm s ⁻¹) | 10 ⁷ | 10 ⁷ | 10 ⁷ |
| Thermal velocity of holes (cm s ⁻¹) | 10 ⁷ | 10 ⁷ | 10 ⁷ |
| Layer density(g cm ⁻³) | 2.328 | 2.328 | 2.328 |
| Auger recombination coefficient for electron(cm ⁶ s ⁻¹) | 2.2x10 ³¹ | 0 | 0 |
| Auger recombination coefficient for hole(cm ⁶ s ⁻¹) | 9.9x10 ⁻³² | 0 | 0 |

| | | | |
|--|-----------------------|---|---|
| Auger recombination coefficient for hole(cm ⁶ s ⁻¹) | 9.9x10 ⁻³² | 0 | 0 |
|--|-----------------------|---|---|

Tableau I: physical parameters of HIT p-substrate

The physical parameters of HIT silicon solar cell with n-type wafer are given in the following table:

| Paramètres | c-Si(n) | a-Si(n) | a-Si(p) |
|--|-----------------------|----------------------|----------------------|
| Thickness | 100µm | 5nm | 5nm |
| Dielectric constant | 11.9 | 11.9 | 11.9 |
| Electron affinity (eV) | 4.05 | 3.9 | 3.9 |
| Bandgap (eV) | 1.12 | 1.72 | 1.72 |
| Effective conduction band density(cm ⁻³) | 2.8x10 ¹⁹ | 10 ²⁰ | 10 ²⁰ |
| Effective valence band density(cm ⁻³) | 2.6x10 ¹⁹ | 10 ²⁰ | 10 ²⁰ |
| Electron mobility(cm ² V ⁻¹ s ⁻¹) | 1041 | 20 | 20 |
| Hole mobility (cm ² V ⁻¹ s ⁻¹) | 412 | 5 | 5 |
| Acceptor concentration(cm ⁻³) | 0 | 0 | 6.8x10 ¹⁹ |
| Donor concentration(cm ⁻³) | 1.5x10 ¹⁶ | 6.8x10 ¹⁹ | 0 |
| Thermal velocity of electrons(cm s ⁻¹) | 10 ⁷ | 10 ⁷ | 10 ⁷ |
| Thermal velocity of holes (cm s ⁻¹) | 10 ⁷ | 10 ⁷ | 10 ⁷ |
| Layer density(g cm ⁻³) | 2.328 | 2.328 | 2.328 |
| Auger recombination coefficient for electron(cm ⁶ s ⁻¹) | 2.2x10 ³¹ | 0 | 0 |
| Auger recombination coefficient for hole(cm ⁶ s ⁻¹) | 9.9x10 ⁻³² | 0 | 0 |

Tableau II: physical parameters of HIT n-substrate

The thin film (5 nm) of a-Si(i) is used for surface passivation between crystalline silicon and amorphous silicon p or n-type in our structure.

The structure of heterojunction with intrinsic silicon solar cell p and n-type wafer are shown in figure 1.

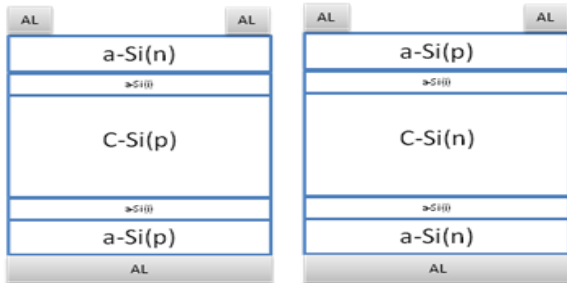


Fig.1. Structure of HIT silicon solar cell p and n-type

In order to simulate the current characteristic or current density as a function of the voltage ($J-V$), a configuration is appropriate for the simulation conditions (solar spectrum AM1.5, illumination = 100 mW /cm², temperature of 27 ° C).

4. Results

Figure 2 shows the band diagram of HIT solar cell with p-type substrate:

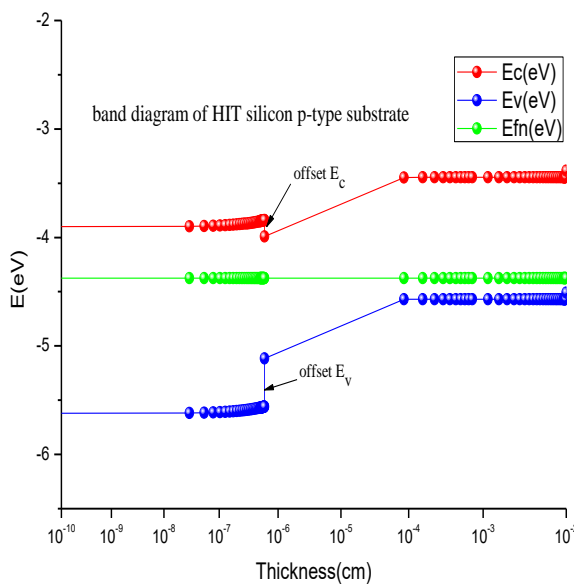


Fig.2. band diagram between a-Si(n) and c-Si(p) of HIT silicon solar cell.

The band offsets of E_c and E_v at interface between a-Si(n) and c-Si(p) are presented in figures (see fig2 and 3) and their value are:

$$\text{Offset } E_c=0,15 \text{ eV.}$$

$$\text{Offset } E_v=0,45 \text{ eV.}$$

$$\text{Offset } E_c + \text{ offset } E_v = E_g^{a\text{-Si}} - E_g^{c\text{-Si}}. [11]$$

Figure 3 shows the band diagram of HIT solar cell with n-type:

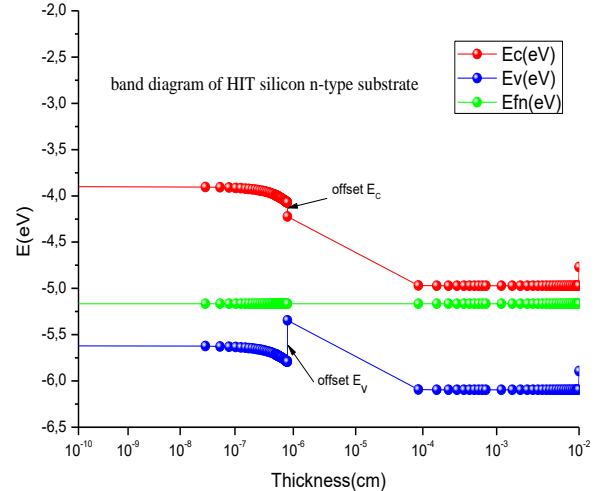


Fig.3. band diagram between a-Si(p) and c-Si(n) of HIT silicon solar cell.

The boundary conditions used in our simulation to plot $J-V$ characteristic are as follows:

Electrical potential is set zero at the front contact.

External voltage V_{ext} it varied in the range of [0, 0,9V] with a pitch of 0,0230V.

The simulation is carried under STC conditions in DC_MOD:

Front illumination with ASTM G173_AM1.5.

Absolute temperature T=300K.

Figure 4 shows the simulation results for the $J-V$ and $P-V$ characteristics of HIT silicon solar cell with p-type wafer:

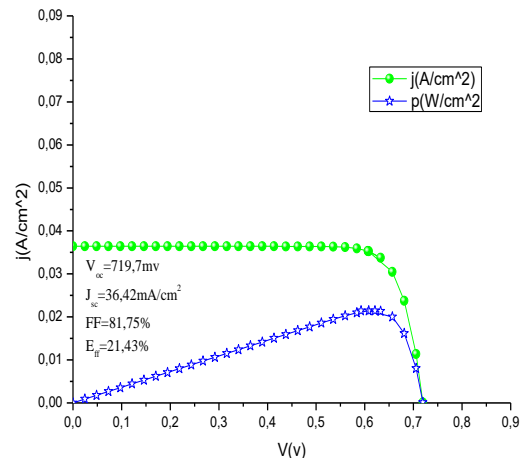


Fig.4. J-V and P-V characteristics of HIT silicon p-type substrate.

The electrical performances of HIT silicon solar cell with p-type substrate are:

Open circuit voltage $V_{oc}=719,7$ mV.

Short circuit of current density $J_{sc}=36,42$ mA/cm².

Fill factor FF=81,75%.

Conversion efficiency $E_{ff}=21,43\%$.

Figure 5 shows the simulation results for the J-V and P-V characteristics of HIT silicon solar cell with n-type wafer:

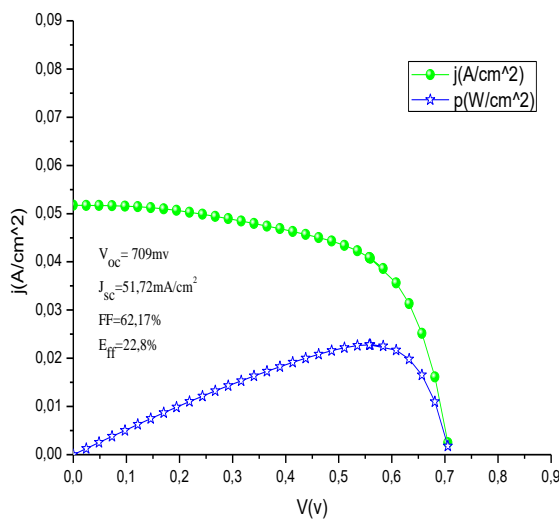


Fig.5. J-V and P-V characteristics of HIT silicon n-type substrate.

The electrical performances of HIT silicon solar cell with n-type substrate are:

Open circuit voltage $V_{oc}=709$ mV.

Short circuit of current density $J_{sc}=51,72$ mA/cm².

Fill factor FF=62,17%.

Conversion efficiency $E_{ff}=22,8\%$.

The spectral response (SR) makes it possible to evaluate the quantum efficiency of a solar cell as a function of the wavelength of the incident light. This measure consists of illuminating the solar cell with a monochromatic spot which is varied in the absorption range between 300 and 1100 nm for the crystalline silicon.

Figure 6 shows the simulation results for the spectral response of HIT silicon solar cell with p and n-type wafer.

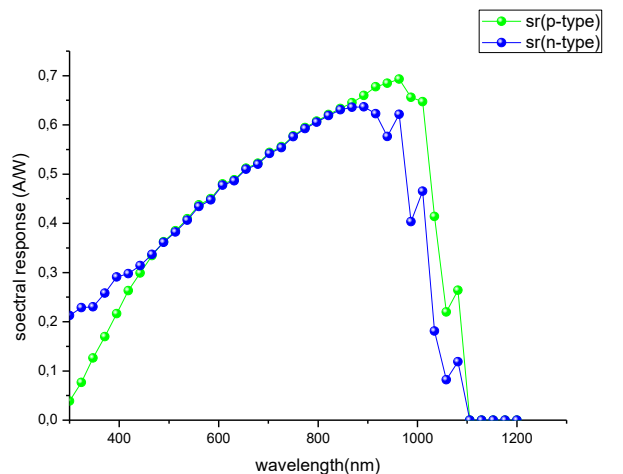


Fig.6. spectral response of HIT silicon p and n-type substrate.

The external and internal quantum efficiency thus gives the percentage of electrons participating in the photocurrent in relation to the number of photons that have actually been absorbed in the cell[12].

Figure 7 shows the external quantum efficiency of HIT solar cell with p and n-type wafer:

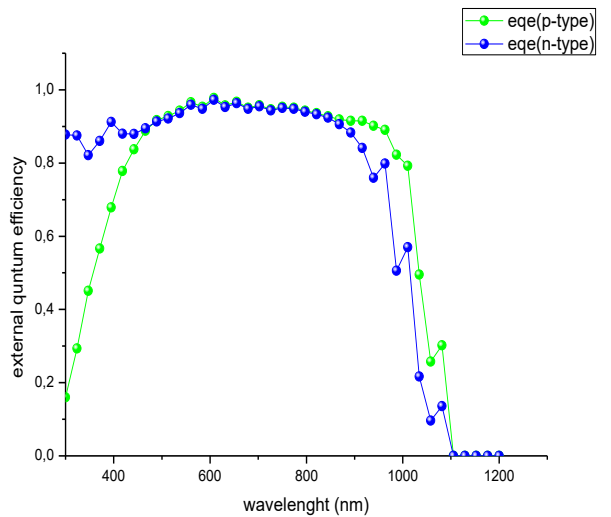


Fig.7. external quantum efficiency

Figure 8 shows the internal quantum efficiency of HIT solar cell with p and n-type wafer:

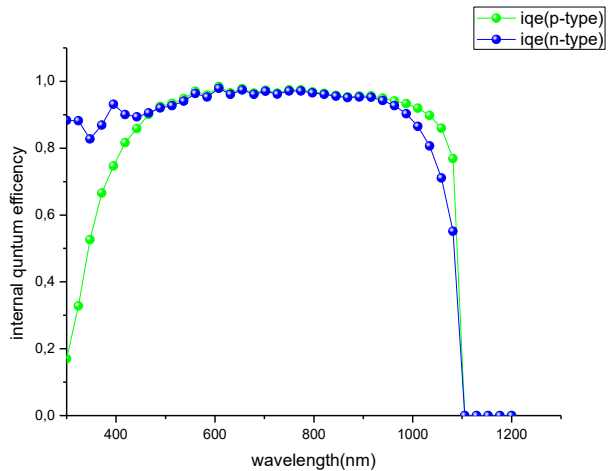


Fig.8. internal quantum efficiency

In the range of the short wavelength (UV), the HIT silicon solar cell with n-type has better light absorption compared to HIT silicon solar cell with p-type (see figure 7 and 8).

5. Conclusion

In our work by numerical simulation we obtained a good and high photovoltaic efficiency conversion (up 20%) whether for heterojunction with intrinsic silicon solar cell p or n-type. On the other hand HIT with p-type wafer achieved a good fill factor is about 81.75%, compared a HIT n-type wafer (62.17%).

References

- [1]. P. P. Altermatt, "Models for numerical device simulations of crystalline silicon solar cells - A review," *J. Comput. Electron.*, vol. 10, no. 3, pp. 314–330, 2011.
- [2]. P. Rapin, "Méthode des éléments finis," *Téchniques de l'ingénieur*.
- [3]. S. Edition, *Photovoltaic Science Handbook of Photovoltaic Science*. 2011.
- [4]. T. Mishima, M. Taguchi, H. Sakata, and E. Maruyama, "Development status of high-efficiency HIT solar cells," *Sol. Energy Mater. Sol. Cells*, vol. 95, no. 1, pp. 18–21, 2011.
- [5]. M. Taguchi *et al.*, "24.7% Record efficiency HIT solar cell on thin silicon wafer," *IEEE J. Photovoltaics*, vol. 4, no. 1, pp. 96–99, 2014.
- [6]. E. Maruyama *et al.*, "Sanyo's challenges to the development of high-efficiency HIT solar cells and the expansion of HIT business," *Conf. Rec. 2006 IEEE 4th World Conf. Photovolt. Energy Conversion, WCPEC-4*, vol. 2, pp. 1455–1460, 2007.
- [7]. M. S. R. Stangl, M. KRIEGEL, "afors-het, a numerical pc-program for simulation of (thin film) heterojunction solar cells, version 2.0 (open-source on demand), to be distributed for public use," vol. 0, pp. 2–5.
- [8]. R. Stangl, C. Leendertz, and J. Haschke, *Numerical Simulation of Solar Cells and Solar Cell Characterization Methods: the Open-Source on Demand Program AFORS-HET*, no. February. 2010.
- [9]. A. Froitzheim, R. Stangl, L. Elstner, M. Kriegel, and W. Fuhs, "AFORS-HET: A COMPUTER-PROGRAM FOR THE SIMULATION OF HETEROJUNCTION SOLAR CELLS TO BE DISTRIBUTED FOR PUBLIC USE."
- [10]. Shin Min , K. (2015). Improvements in Newton-Rapshon Method for Nonlinear Equations Using Modied Adomian Decomposition Method. International Journal of Mathematical Analysis, 9(39), 1919-1928..
- [11]. L. Shen, F. Meng, and Z. Liu, "Roles of the Fermi level of doped a-Si: H and band offsets at a-Si: H/c-Si interfaces in n-type HIT solar cells," *Sol. Energy*, vol. 97, pp. 168–175, 2013.K. W. J. , B. (1990). A new approach to high-efficiency multi-band-gap solar cells,. *J. Appl. Phys.*, 67, 3490-3493.